Numerical Solution of the Two-Dimensional Premixed Laminar Flame Equations

S. L. Aly,* R. B. Simpson,† and C. E. Hermance‡
University of Waterloo, Waterloo, Ont., Canada

The present paper presents a numerical solution method for the two-dimensional elliptic partial differential equations modeling a premixed laminar flame freely propagating at constant pressure between parallel plates having a constant, cool wall temperature. The technique developed is an efficient, semidirect (semi-iterative) method termed "multistep damped Picard iteration." Picard linearization of the nonlinear terms together with variable damping as the solution progressed and a sparse matrix elliptic solver allowed rapid solution to be obtained as a limit of a convergent sequence of solutions. The flame-quenching limit was determined by iterating the solution with respect to the distance separating the plates and approaching the limit state to within a specific criterion. Global kinetics and average transport properties were used for a simulated propane-air mixture; radiation loss was neglected throughout the analysis. The method was used to study the effect of the "ignition temperature" on the flame parameters as well as to reveal the two-dimensional structure of the flame at the quenching limit.

Nomenclature

A = cross-sectional area, Sec. IV B, cm^2
c_p = specific heat at constant pressure of the mixture, cal/g K
D = diffusion coefficient for the fuel species cm^2/s
D_e = hydraulic (equivalent) diameter of the parallel plates, cm
E = activation energy, cal/mole
G = mass flow rate (mass burning rate), g/cm^{2}s; eigenvalue of the flame equations
H_c = heat of combustion of the fuel, cal/g
k = frequency factor (reaction rate constant), units depend on reaction order
L = distance separating the parallel plates, cm
m = reaction order
P = perimeter, Sec. IV B, cm
p = pressure, atm
Pe = quenching Peclet number
QD = quenching distance, cm
R = universal gas constant, 1.986 cal/mole K
S_0 = surface of the upstream boundary, cm^2, Sec. III B
S_{out} = surface of the downstream boundary cm^2, Sec. III B
T = temperature, K
T_i = ignition (cutoff) temperature, K
T_0 = ambient temperature, K
u = x component of the mixture velocity, cm/s
V = volume in Sec. III B cm^3
= flame speed in Eq. (22), cm/s
v_{out} = velocity of the mixture at the downstream boundary ($\perp$ to S_{out}), cm/s
w = rate of consumption of fuel per unit volume and time, g/cm^3 s
Y = mass of reactant (fuel) per unit mass of mixture
Y_0 = mass of reactant (fuel) in unburned mixture per unit mass of that mixture
α = Y/Y_0
λ = thermal conductivity of the mixture cal/cm s K
ρ = local mixture density, g/cm^3
ρ_0 = density of unburned mixture, g/cm^3
ρ_{out} = density of the mixture at the downstream boundary, Sec. III B

Subscript

0 = upstream boundary (reactants or cold)

Received May 4, 1978; revision received Aug. 21, 1978.

Index categories: Computational Methods; Combustion and Combustor Designs; Combustion Stability, Ignition, and Detonation.

*Postdoctoral Fellow, Dept. of Mechanical Engineering, Thermal Engineering Group.

†Associate Professor, Dept. of Computer Sciences.

‡Professor of Mechanical Engineering, Thermal Engineering Group. Member AIAA.

I. Introduction

THE majority of the numerical work done in the area of laminar flame theory has been confined to the one-dimensional adiabatic system, primarily because of the complexity of the differential equations describing this type of flame. This complexity lies essentially in the severe nature of temperature nonlinearity of the Arrhenius reaction rate term and the eigenvalue feature of the flame velocity.

Several numerical approaches have been used to tackle this one-dimensional adiabatic system. Hirschfelder et al.[1] used the straightforward shooting technique to study the structure and burning velocity of hydrazine, nitric oxide, and ozone flames. Unfortunately, only the simplest problems are solvable in such a manner. Spalding et al.[2,3] integrated the time-dependent conservation equations by the standard explicit finite-difference technique and obtained the steady-state laminar flame solution as a limit of a convergent sequence of solutions in time. This approach was shown by Dixon-Lewis[4] to be more capable of handling systems with many reactions and species. Bledjian[5] followed the same approach, but solved the time-dependent equations using the method of lines. More recently, Wilde[6] suggested solving the flame equations as a boundary-layer problem, using Newton linearization to linearize the nonlinear reaction term.

However, all the one-dimensional adiabatic flame models were unable to exhibit the experimentally observable quenching limit, which is the value of the tube diameter (quenching diameter) or the distance separating the parallel plates (quenching distance) below which the flame cannot propagate. This occurs because of the conductive heat loss to the containing walls in a direction normal to that of flame propagation. Thus it is apparent that the actual process of flame propagation in cylindrical tubes or between parallel plates with fixed cool wall temperature is a two-dimensional process. Despite this fact, previous nonadiabatic models, e.g., 13, 14, 16, accounted for the conductive heat loss to the wall by assuming a volumetric heat loss in the energy equation and

the numerical approach followed was essentially that of Ref. 1.

Virtually no numerical work was done in the area of multidimensional laminar flame theory except that of von Karman and Millan[7] and Penner.[8] The former work dealt with studying the thermal behavior of the flame near a cold wall. However, the burning velocity was considered an a priori known quantity and no extinction limit was obtained. Penner[8] made the same assumption regarding the flame speed and solved the two-dimensional elliptic PDE, modeling an adiabatic inverted flame, using a point successive overrelaxation iterative scheme equipped with the projection method to control the nonlinear terms.

In the present paper, an efficient solution technique to solve the two-dimensional elliptic PDE, modeling the free propagation of laminar flame between parallel plates is described. The solution yields the flame speed eigenvalue and the internal structure of the flame under study at any distance separating the plates. Moreover, the method possesses the mechanism necessary to determine the limiting quenching solution.

II. The Mathematical Formulation

The physical model is that of a laminar flame propagating between parallel plates at a speed, relative to the unburned mixture, equal to the burning velocity or flame speed. Adopting a coordinate system traveling with the wave, the flame zone is stationary relative to the observer and the explosive mixture is flowing by. The unburned combustible mixture streams in the positive x direction; far upstream of the flame region, the mixture approaches the flame wave with the laminar flame speed. While passing through the flame the reactants in the mixture are generally consumed and products of combustion are produced. The temperature in the stream increases from that of the unburned mixture T_0 at the cold (upstream) boundary to a certain maximum temperature and then falls off gradually far downstream to T_0 again as a result of the wall cooling effect.

A. Equations and Boundary Conditions

The set of conservation equations applicable to a general system of chemically reacting flow is given in some references such as Ref. 9. However, these equations are not commonly applied in their most general form to the laminar flame system since several assumptions pertinent to this system are made. These assumptions range from the neglect of body forces, viscous effects, ordered kinetic energy, and pressure-gradient diffusion as well as Soret and Dufour effects, to considering the gas mixture as ideal, the binary diffusion coefficients of all pairs of species equal, and that steady state prevails (see Ref. 10). Further assumptions are: 1) constant and equal specific heats for all species, equal to the average specific heat of the mixture; 2) the y component of the mixture velocity is neglected; 3) the radiation loss to the surroundings is neglected.

Making use of the previous assumptions, the overall continuity is satisfied by

$$\rho u = G = \text{constant} \tag{1}$$

The momentum equation for low-speed flow reduces to

$$p \approx \text{constant} \tag{2}$$

which is the usual approximation in deflagration waves. At this point, it is important to note that if one drops assumption 2 it would also be necessary to solve the momentum equation numerically.

Before deducing the energy and mass species conservation equations, two additional simplifying and nonessential assumptions regarding the transport properties are made: 4) the variation of thermal conductivity, λ, with temperature is ignored and only an average value is considered; 5) the diffusion coefficient D varies linearly with temperature.

With the above assumptions the energy equation in two dimensions reduces to

$$\frac{\partial^2 T}{\partial x^2} + \frac{\partial^2 T}{\partial y^2} - \frac{Gc_p}{\lambda}\frac{\partial T}{\partial x} = -\frac{1}{\lambda} H_c |w| \tag{3}$$

The species conservation equations reduce to only one equation pertaining to the fuel species because of the global kinetics model adopted presently and described later, i.e.,

$$LeY_0 \frac{\partial^2 \alpha}{\partial x^2} + LeY_0 \frac{\partial^2 \alpha}{\partial y^2} - \frac{Gc_p}{\lambda} Y_0 \frac{\partial \alpha}{\partial x} = -\frac{c_p}{\lambda} w \tag{4}$$

where Lewis number is defined as

$$Le = \rho c_p D/\lambda \tag{5}$$

It is to be noted that assumption 5 has been adopted so that Le will be constant with respect to temperature variation using averaged thermal properties.

The last assumption to be made is related to the y component of the mass diffusion and is not generally very obvious: 6) the mass diffusion of the various species in the y direction is ignored.

This last assumption finds some of its justification in the experimentally observed fact that the nature of the surface does not have any pronounced effect on quenching. More importantly and less obviously is the physical picture that arises if the transverse diffusion were allowed while retaining assumption 2 and considering the wall chemically inert. It can be expected, based on physical grounds and preliminary numerical integration of Eqs. (3) and (4), that the reactants species passing near the wall are virtually unconsumed because of the cooling effect of the wall and the consequent cessation of chemical reactions. The unreacted species will diffuse towards the hotter (interior) regions (perhaps before it cools enough) and chemical reactions will start again behind the original wave front, resulting in a small distributed heat release behind the main flame zone. Thus we can expect a kind of extended diffusion flame to trail the premixed laminar flame front. This expected physical picture is outside the realm of a strict laminar flame front propagating between parallel plates considered herein. Furthermore, this reacting diffusion may, in general, induce a bulk mass flow which is neglected by assumption 2, therefore consistency demands assumption 6.

Employing assumption 6, Eq. (4) becomes

$$Le\, Y_0 \frac{\partial^2 \alpha}{\partial x^2} - \frac{Gc_p}{\lambda} Y_0 \frac{\partial \alpha}{\partial x} = -\frac{c_p}{\lambda} w \tag{6}$$

Concerning the boundary conditions applicable in the y direction, it is assumed that the walls of the plates remain at room temperature; thus at

$$y = 0 \quad T = T_0, \quad \text{for all } x \tag{7}$$

and

$$y = L/2 \quad \partial T/\partial y = 0, \quad \text{for all } x \tag{8}$$

Equation (8) reflects the required symmetry across the centerline of the duct.

As for the x direction, the boundary conditions applicable at the cold boundary are the same as for the adiabatic case, that is at

$$x = -\infty, \quad 0 \le y \le L/2 \qquad T = T_0$$

$$\partial T/\partial x = 0, \quad \text{i.e., no heat source or sink}$$

$$\alpha = 1 \tag{9}$$

The cold boundary difficulty is handled through letting the reaction rate function vanish for temperatures less than a certain "ignition temperature," T_i. The downstream boundary conditions are at

$$x=+\infty, \quad 0\leq y\leq L/2$$

$$\partial T/\partial x=0, \quad \partial\alpha/\partial x=0 \tag{10}$$

Discussion has occurred among some research workers[11-14] regarding whether the fuel is fully depleted or not at the downstream boundary. In the present formulation, the picture is generally clearer in that the fuel concentration at $x=+\infty$ is, in general, a function of the transverse direction. Accordingly, the appropriate downstream boundary condition for α should be of the Neumann type, expressing the physical nonexistence of mass sources or sinks at infinity. Another important virtue of adopting this kind of boundary condition is indicated later (Sec. III E).

B. Reaction Kinetics

The present paper deals with the combustion of a hydrocarbon (propane)-air mixture within the framework of global kinetics, which ignores the actual mechanism of reaction and considers the reaction taking place in a single step between the fuel and oxidant according to the following equation

$$f+O+M\rightarrow P+M \tag{11}$$

where f, O, P and M symbolize the fuel, oxidant, combustion products, and inert diluent species, respectively. The reaction rate function is of the Arrhenius type and takes the following form

$$w=-k\left(\frac{\alpha Y_0\rho_0 T_0}{T}\right)^m e^{-E/RT}$$

$$w=0, \qquad \text{for } T<T_i \tag{12}$$

where m is the order of reaction. The actual global reaction order is somewhere between 1 and 2 and is taken here as equal to 1 for somplicity.[15]

C. Numerical Data

The numerical values of the various physical properties have been chosen to simulate and represent the stoichiometric propane-air system. E, H_c, ρ_0, c_p, and λ are respectively taken to be (Ref. 16) 40,000 cal/mole, 1.11×10^4 cal/g propane, 1.3×10^{-3} g/cm^3 for the one atmosphere pressure, 0.32 cal/g K, and 1.6×10^{-4} cal/cm Ks. The reaction rate constant k is taken to be 0.175×10^{10} s^{-1} for a first-order reaction. This value was chosen to yield a flame speed at $L=5$ cm equal to approximately 45 cm/s at $Le=0$. For the stoichiometric propane-air mixture, Y_0 is taken to be 1/16.5. The ambient temperature is considered 300 K throughout the whole analysis.

III. The Solution Method

Equations (3) and (6), with their associated boundary conditions, and Eq. (12) were integrated numerically using a finite-difference method.

A. Discretization of the Field

In order to accommodate the nature of the laminar flame solution where a very steep rise in temperature occurs over a small distance, while the heat release rate is simultaneously increasing, the whole preceded by an asymptotic temperature rise above the ambient temperature and followed by a gradual cooling off in the after burning region, a variable mesh size in the x direction was employed. The integration domain was split into three regions with typical values of mesh size, Δx, 0.05, 0.2×10^{-2}, and 0.1 cm in the three sections, respectively, for the case of first-order stoichiometric kinetics with $Le=0$.

It is to be noted that the introduction of a variable mesh size field is not essential per se, and was introduced simply to cut down the number of grid points used. We found 100 grid points in the x direction to be adequate.

As for the y direction, ten grid points were used from the wall to the centerline of the duct. This led to a mesh size in the transverse direction, Δy, dependent on the distance separating the plates in a manner satisfying the physical picture of the problem, being large where the temperature gradients are not steep (at large L's) and getting smaller with decreasing L where the effect of the wall (and consequently the two-dimensionality effect) increases.

The boundary conditions were imposed at a sufficiently large distance away from the flame. The general method of determining the validity of the solution obtained over such a limited field, which represents the originally infinite field, is to repeat the integration for successively larger fields and see whether significant changes occurred. They did not.

B. Eigenvalue Determination

In general, the solution technique of the laminar flame problem needs to be equipped with a kind of systematic device or mechanism whereby one can determine the flame speed. This device should be amenable to application in both one- and multidimensional flame problems, as well as with the various methods employed to solve the system of equations. It seems that the necessary mechanism can be achieved by relating the flame speed to the structure of the flame through the macroscopic mass balance of one of the reactants (e.g., the fuel) in the fresh mixture.

The mathematical formulation of such a balance can, in general, be written for the control volume containing the flame as follows:

$$\iiint_V |w|\,dV=u_0\iint_{S_0}\rho_0 Y_0\alpha_0\,dS_0$$

$$-\iint_{S_{out}}\rho_{out}\alpha_{out}Y_0 v_{out}\,dS_{out} \tag{13}$$

Equation (13) is used to express the laminar flame speed u_0 in terms of the flame structure as follows

$$u_0=\frac{\iiint_V |w|\,dV+\iint_{S_{out}}\rho_{out}\alpha_{out}Y_0 v_{out}\,dS_{out}}{\iint_{S_0}\rho_0 Y_0\alpha_0\,dS_0} \tag{14}$$

This relation reflects the physical picture of the continuous feeding of fresh charge to the flame wave, at a rate equal to the mass burning velocity, to compensate for the consumption of fuel by chemical reactions. Accordingly, it appears physically more meaningful to use relation (14), whenever a value for the flame speed is needed, while a solution is being computed.

In the present analysis, Eq. (14) was conveniently rearranged to take the following form for G

$$G=\iint |w|\,dx\,dy\Big/\left[y_0\frac{L}{2}-Y_0\int_0^{L/2}\alpha(\infty)\,dy\right] \tag{15}$$

Note that use has been made of the upstream boundary condition, namely $\alpha=1$, and of Eq. (1) in deriving Eq. (15).

With Eq. (15), expressing G in terms of T and α, it is possible to eliminate G from Eqs. (3) and (6), and view the laminar flame formulation alternatively as a system of integropartial differential equations; but in this event, the eigenvalue feature of the problem is lost. The view adopted in the present analysis is to leave Eqs. (3) and (6) containing G as an eigenvalue (a parameter to be determined from the solution), and look upon Eq. (15) as a constraint to be applied on G while a solution is being worked out. Parenthetically, it may be noted that in the more general case where the y component of the velocity is taken into consideration, the flame speed does not appear in the equations but rather in the boundary conditions and the approach adopted here is still applicable.

C. The Solution Technique: "Multistep Damped Picard Iteration"

For the problem at hand it can be expected in advance that Lieberstein's[17] method of nonlinear successive overrelaxation would be very slow since it is essentially a point iterative technique. Moreover, the overrelaxation parameter employed in this method can be anticipated to drive a severely nonlinear system like that of the laminar flame equations towards instability. It has been shown by Penner[8] to be unstable when solving the two-dimensional inverted laminar flame equations. As a result, Penner used the projection method to control the nonlinearity in the system along with a point successive overrelaxation technique as indicated in Sec. I. However, Penner's method proved unsuccessful in coping with the equations of the present study.

Adopting a more formal approach, the technique established to solve Eqs. (3) and (6) with the associated boundary conditions and Eq. (15) is a semidirect computation method. It is an iteration scheme, employing a direct elliptic solver that covers all the computational field at each step; we term it "multistep damped Picard iteration." The essence of the method is to linearize the nonlinear terms in the differential equations using Picard's method; the final solution is obtained by a convergent sequence of damped solutions of the linearized system, the damping being effected differently at various stages as the iteration proceeds. The notion of underrelaxing the iteration in steps was invoked to enable the scheme to overcome the small oscillations observed in G whenever the solution was approached. In addition, it makes the scheme more able to deal with crude initial estimates of temperature and species concentration efficiently. Typically, three stages were used with damping parameters 1, 0.4, and 0.2, respectively. However, the idea is general, and can be effected differently regarding the values of the parameters and the length of each stage, depending on the particular case under study.

The initial estimates of the temperature and fuel concentration were rather crude and did not need any prior knowledge of the solution. The initial temperature field was assumed to be a spike of 2300 K extending typically over four grid points in the x direction (in the middle section) and all the grid points in the y direction. Elsewhere the temperature was assumed equal to the ambient temperature. Extension of the spike to all the interior points on the y direction was necessitated by our neglect of the y component of the mixture velocity, which made the wave unable to propagate transversely. As for the α distribution, it was assumed initially independent of y, taking on the value of unity up to the beginning of the temperature spike, then a linear variation from one to zero across the spike, and afterwards zero everywhere.

Picard linearization was used rather than the more efficient Newton linearization because it produced a linearized separable elliptic PDE for Eq. (3), for which a sparse matrix direct solver was already available.[18] In the present problem, using Newton's method together with a point successive overrelaxation (SOR) linear solver proved inferior in terms of efficiency to the one finally adopted.

Picard linearization of Eq. (3) yields the following form

$$\frac{\partial^2 T^{K+1}}{\partial x^2}+\frac{\partial^2 T^{K+1}}{\partial y^2}-G(T^K,\alpha^K)\frac{c_p}{\lambda}\frac{\partial T^{K+1}}{\partial x}$$

$$=-\frac{1}{\lambda}H_c k\left(\frac{\alpha^K Y_0\rho_0 T_0}{T^K}\right)e^{-E/RT^K} \tag{16}$$

where K is the iteration index.

Equation (6) is linear in α and can be written as follows:

$$LeY_0\frac{\partial^2\alpha^{K+1}}{\partial x^2}-G(T^{K+1},\alpha^K)\frac{c_p}{\lambda}Y_0\frac{\partial\alpha^{K+1}}{\partial x}$$

$$-\frac{c_p}{\lambda}k\left(\frac{Y_0\rho_0 T_0}{T^{K+1}}\right)e^{-E/RT^{K+1}}\alpha^{K+1}=0 \tag{17}$$

For the case of $Le=0$, the first term in Eq. (17), containing the second derivative of α, is knocked out and the equation becomes first order and parabolic. Consequently, the downstream boundary condition for α does not have to be imposed any longer and a marching technique was used to solve the fuel concentration equation.

Equation (16) was discretized by replacing the second derivatives by their central finite-difference forms. For the points lying at the interface between two different mesh sizes, e.g., Δx_1 and Δx_2, the second derivatives were replaced by the following second-order finite-difference analog[19]

$$\frac{\partial^2 T}{\partial x^2}=\frac{2}{r(r+1)}\frac{rT_{i+1,j}-(1+r)T_{i,j}+T_{i-1,j}}{(\Delta x_2)^2} \tag{18}$$

where $r=\Delta x_2/\Delta x_1$. Central differencing was used to replace the first derivative in the energy equation at any grid point in the middle section and upwind differencing was used for the grid points lying in the first and third sections, where the longitudinal mesh size was relatively large, as well as the points lying at the interface between two different mesh sizes. It is noteworthy that using central differencing for the first derivative in the first and third sections made no difference for the cases studied here.

Equation (17) with $Le=0$ was discretized by using stiffly stable backward differencing[20] to approximate the first derivative since the marching technique is susceptible to instability. The marching equation takes the following form

$$\alpha_{i,j}^{k+1}=\frac{1}{1+k\dfrac{\rho_0 T_0}{T^{k+1}}\Delta x\dfrac{1}{G(T^{K+1},\alpha^K)}e^{-E/RT^{K+1}}}\alpha_{i-1,j}^{k+1} \tag{19}$$

The computing algorithm is generally describable as follows:

1) Initially assume arbitrary temperature and species concentration distributions throughout the field, T^K and α^K.

2) Calculate $G(T^K,\alpha^K)$ using Eq. (15) by numerically carrying out the integrations involved.

3) Solve the set of discretized energy equations to produce the temperature field $\bar{T}^{K+1}$. Solution is via the linear solver "POIS."[18]

4) Compute a new, generally underrelaxed, temperature field T^{K+1} according to the relation

$$T^{K+1}=T^K+\nu(\bar{T}^{K+1}-T^K) \tag{20}$$

where $\nu(\nu\leq 1)$ is in general an underrelaxation parameter whose value depends on the particular stage of iteration.

5) Use T^{K+1} and α^K to numerically compute $G(T^{K+1},\alpha^K)$ through Eq. (15) again.

6) Employing Eq. (19), march down the computational field from the upstream boundary to calculate α^{K+1}.

7) Steps 2-6 are repeated until the convergence criterion, namely

$$(T^{K+1}-T^{K})/T^{K+1}\leq\epsilon \tag{21}$$

is met. Since the major concern of the present work was the development of the solution method rather than obtaining accurate numerical results, ϵ was taken to be 0.01.

The final values of T^{K+1} and α^{K+1} provide the solution to the problem at a certain L; G is then calculated using these values and the flame velocity is obtained by dividing ρ_0 into G.

When $Le\neq 0$, it is not possible, in general, to apply the marching technique to the mass species equation and a boundary-value direct solver, such as, e.g., the Thomas algorithm,[19] may be used in Step 6 in the previous computational procedure.

D. Comments Related to the "Multistep Damped Picard Iteration"

The above-described technique was successful in solving the differential equations of the problem efficiently. The number of iterations needed for convergence changed with the various conditions of the problem resulting from varying L. Typical values ranged from about 10 iterations with $L=5$ cm to, at times, as high as 40 iterations for some conditions near the limiting solutions. At $L=1$ cm, 19 iterations were required for $T_i=700$, 1000 K; 15 iterations were needed for $T_i=1500$, 1900 K. In terms of computational time, compilation and execution, values ranging from 30 to about 50 s were typical, depending on L, using Fortran "H" and an IBM 360/75 computer.

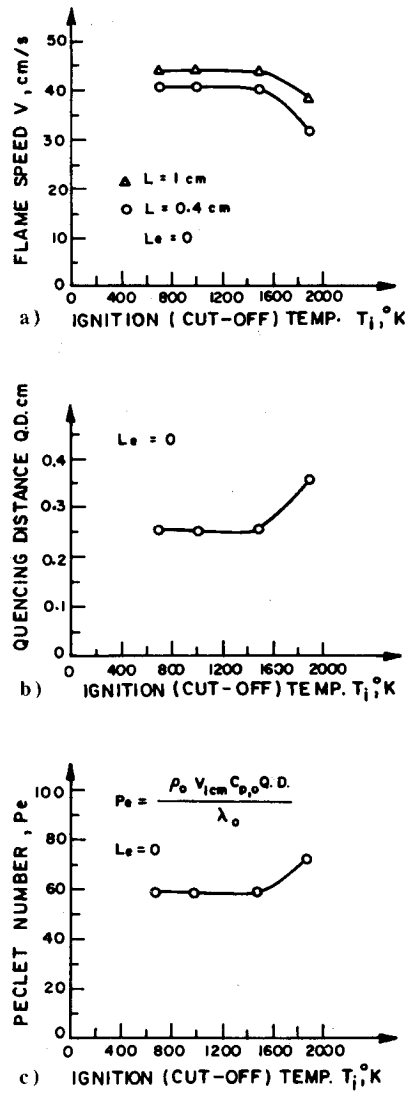

Fig. 1 a) Variation of flame speed with ignition (cutoff) temperature; b) variation of quenching distance with ignition (cutoff) temperature; c) variation of critical peclet number with ignition (cutoff) temperature.

E. The Limiting Solution

The solution technique is equipped with a straightforward mechanism to determine the limiting solution of the system of equations. Before proceeding with exposing such a mechanism, it is worthwhile to note that $T=T_0$, $\alpha=1$, and $G=0$ constitute a solution (the trivial one) of Eqs. (3) and (6). This solution was made possible only through the imposition of the Neumann-type downstream boundary condition for α. The virtue of this trivial solution is that it corresponds to the condition of no flame propagation. Thus, under no circumstances could a divergent result, with which nonexistence of flame was identified in many previous investigations, be acceptable in the present method.

The determination of the quenching limit solution involved an iteration process for the whole flame solution with respect to L to meet a certain convergence criterion. This included the comparison between the smallest value of the distance separating the plates, L_s, at which a nontrivial solution was obtained and L', at which the solution converged to the trivial one. Convergence was considered achieved in the present analysis when such a difference between L_s and L' was $\leq 2\%$. The solution at the final L_s was taken to be the flame-quenching solution. Precisely, the same procedure can be applied to determine other limiting solutions of the flame equations arising from decreasing the pressure or the initial fuel concentration. The computation time required for convergence to the quenching solution for the present case was about 100 s.

IV. Results of the Computation

The technique just described can be used to study the flame behavior at any given value of L, from large (where a one-dimensional adiabatic theory is found to be appropriate since the flame essentially behaves adiabatically) to small. This technique was used to study the effect of T_i on the flame system at relatively large L ($L=1$ cm) as well as the behavior of the flame with changing L.

A. The T_i Results

Although no rule exists in the literature regarding the value or range of values this "ignition temperature" may take, it has been the common practice to assume it close to the maximum flame temperature.[21] The present study of T_i sheds more light on the nature of this temperature, which was originally introduced to solve what is known as the cold boundary difficulty.

Figures 1a-c show, respectively, the effect of T_i on some of the flame parameters, namely the flame speed, the quenching distance, and the quenching Pe. It is apparent from these figures that the various flame parameters are not affected by the particular choice of T_i up to a certain value, beyond which the flame speed starts decreasing while both the quenching distance and Pe start increasing.

To have additional physical insight into the effects of choosing different values of T_i, the variation of the volumetric heat release rate along the center line of the duct is plotted for $T_i=700$, 1500, and 1900 K in Fig. 2. It can be seen that choosing a high value of T_i, i.e., close to the maximum flame temperature, leads to the neglect of a sizable amount of heat release in the system, which leads to the decrease in flame speed and the increase in quenching distance.

The above results show that the laminar flame solution is independent of the assumed T_i value as long as it falls within a certain range (in the present work from about 700 K to ap-

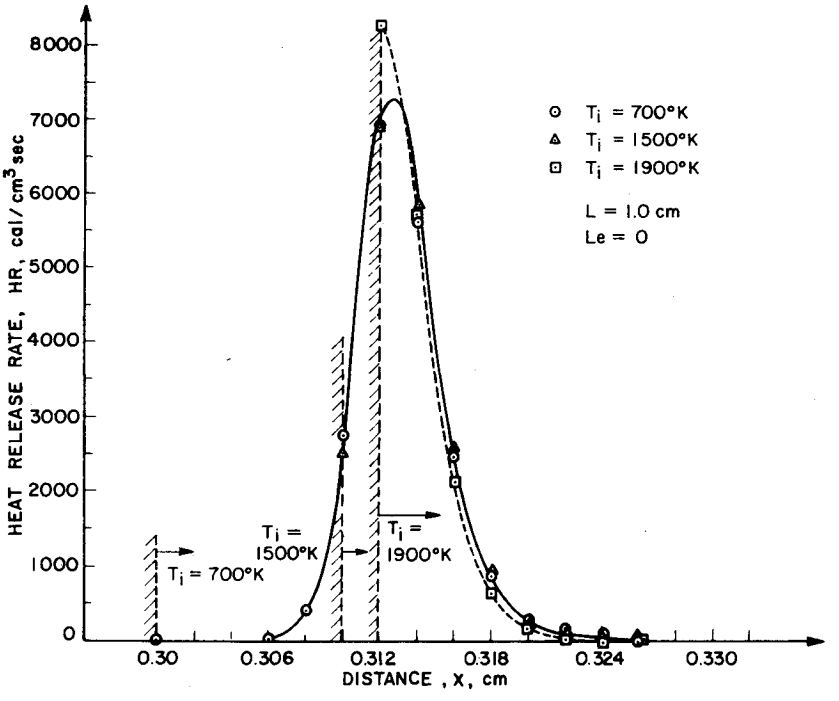

Fig. 2 Variation of heat release rate along the center line of the duct at various ignition (cutoff) temperature.

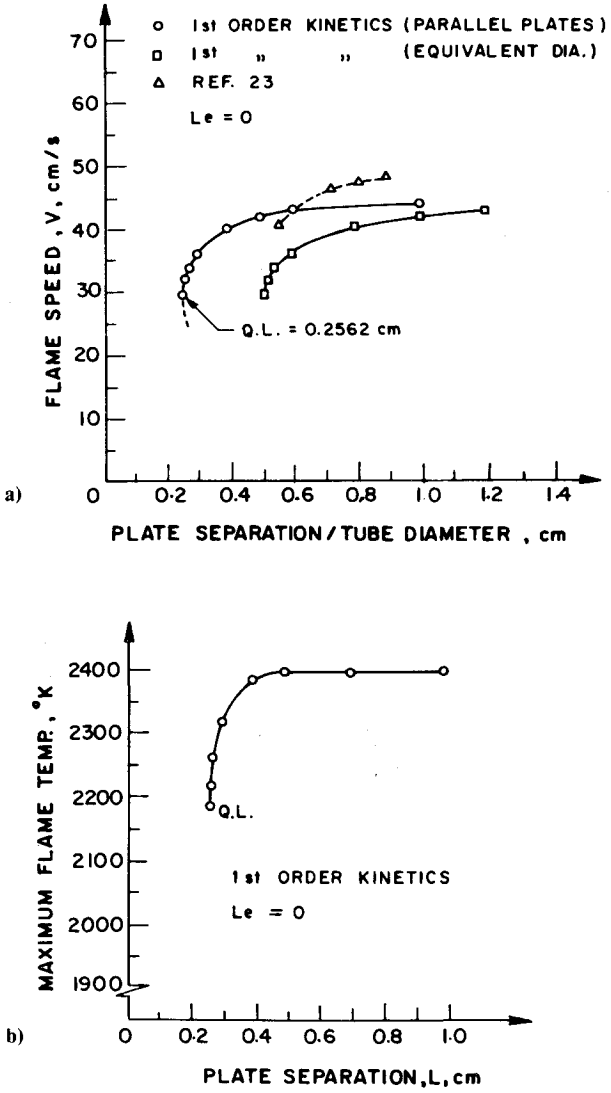

Fig. 3 a) Variation of flame speed with the distance separating the parallel plates or tube diameter; b) variation of maximum flame temperature with plate separation.

proximately 1400 K). Clearly, the appropriate value is rather closer to the ambient temperature than to the maximum flame temperature. This range of T_i indicates that the value of the ignition temperature does not have any real bearing on the laminar flame problem. Furthermore, it does not have any direct relation to the high temperature characterizing the ignition delay in the theory of homogeneous explosions.[22] As a result it is looked upon simply as a necessary mathematical artifice to remedy the cold boundary difficuty. However, it is believed that this temperature possesses some physical significance because it expresses a physically satisfying, real limit for the vanishingly small, but finite, Arrhenius reaction rate at temperatures near the cold boundary temperature. In this light, it seems plausible to consider T_i as a "cutoff" temperature rather than an "ignition temerature."

B. The Stoichiometric Flame at Atmospheric Pressure

The present technique was used to study the variation of various flame parameters with the distance separating the plates. Figures 3a and b show such variation for the flame speed and maximum temperature. Both figures indicate that these flame parameters are not affected appreciably until the quenching limit is approached. The experimental measurement of Payman and Wheeler[23] for the horizontal propagation of the methane-air mixture in the tubes show the same general trend. This is more clearly seen when the parallel plate results are presented in terms of the equivalent diameter, $D_e = 4A/P = 2L$.

The quenching distance for this particular choice of chemical kinetics was calculated to be 0.2562 cm. This is a little higher than the majority of the reported experimental values for the propane-air mixture, which hover about approximately 0.21 cm.[15] This difference may be attributed to the approximate nature of the numerical data chosen to represent the kinetics and transport properties.

A better basis for comparison between the various quenching studies is usually obtained through the quenching Pe defined as

$$\text{quenching } Pe = (\rho_0 V c_{p,0} \mathrm{QD})/\lambda_0 \qquad (22)$$

The "theoretical" quenching Pe was calculated to be approximately 59, based on the thermal diffusivity of the un-

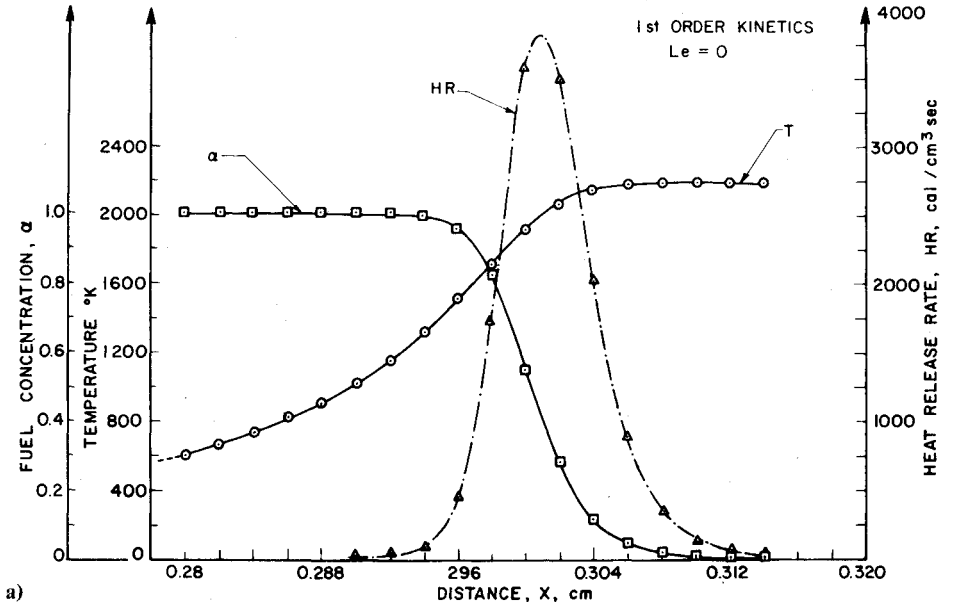

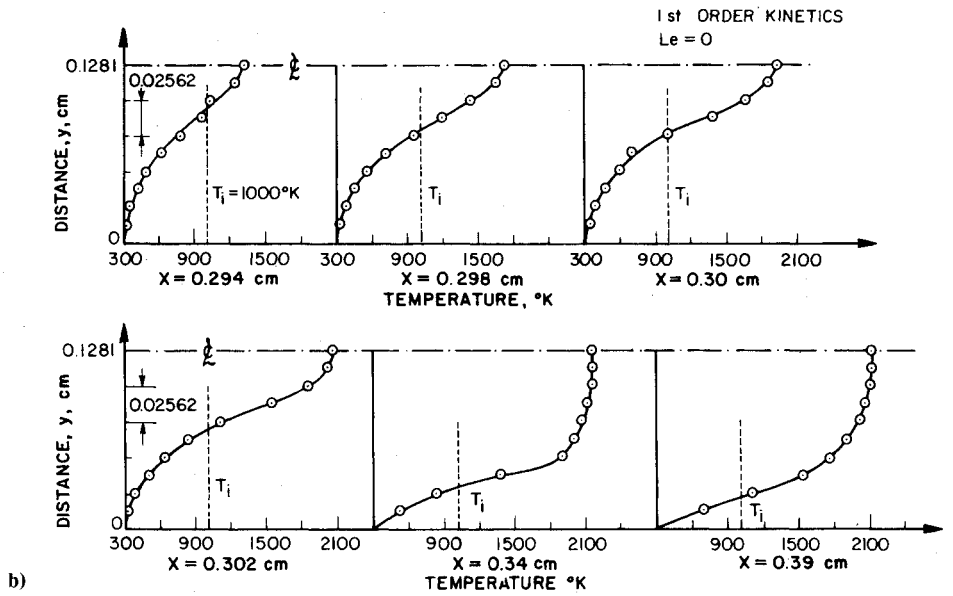

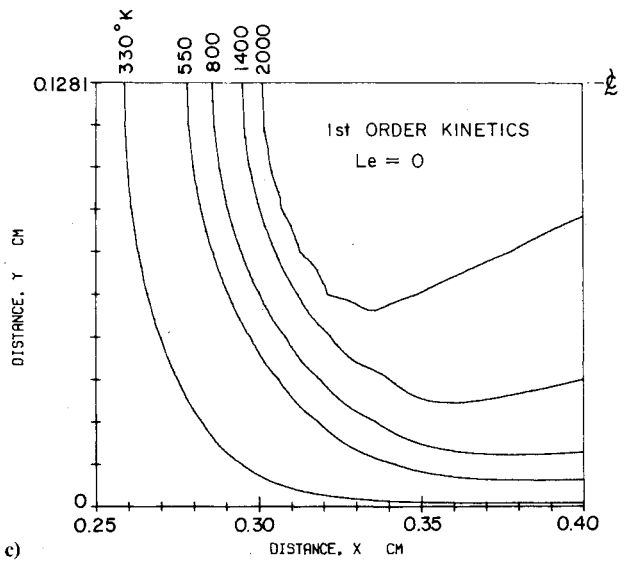

Fig. 4 a) Variation of temperature T, fuel concentration, α, and heat release rate, HR, along the center line of the duct at quenching limit; b) temperature profiles across the duct at various x locations, at quenching limit; c) isotherms of the internal structure of the wave, $L = QD = 0.2562$ cm (computer plotted).

burned mixture and the flame speed at $L=5$ cm. The experimental value is about 45, using an adiabatic laminar flame speed of 41 cm/s[24] for the stoichiometric propane-air mixture at 1 atm, and the same value of thermal diffusivity. The figure provided by Spalding's[25] one-dimensional theory, after having been recalculated by Potter[15] to adjust for typical hydrocarbon data, was 66. Yang's theory,[16] after adjustment to the parallel plate case and with the thermal properties used herein, predicts a quencing $Pe=91$ based on his theoretical adiabatic flame speed at $Le=0$.

The complete picture of the thermal flame structure at the quenching limit is revealed in Figs. 4a-c. The temperature profiles of the flame across the duct clearly show the two-dimensional aspect of the flame-quenching phenomenon. The isotherms in Fig. 4c easily reveal the extent of the penetration of the cool region inside the duct.

V. Conclusions

A number of important conclusions can be drawn from the results just presented. They are as follows.

1) Applying the Neumann boundary conditions for the downstream fuel concentration provides a meaningful formulation of the laminar flame problem. The equations then exhibit extinction phenomena by allowing a trivial solution to the equations to exist, which corresponds to the extinguished state.

2) The described numerical technique (multistep damped Picard iteration) is a powerful semidirect boundary value solution for the flame equations. The mechanism incorporated in the solution method to handle the eigenvalue provides for its systematic evaluation.

3) The multistep damping technique is capable of coping with the severely nonlinear Arrhenius temperature dependence and, at the same time, crude initial estimates of the dependent variables efficiently.

4) It has been shown that the temperature used to circumvent the "cold boundary" difficulty is better regarded as a reaction "cutoff" temperature than as an "ignition" temperature, and that the flame has a strongly two-dimensional character as the quenching is approached.

5) Finally, we conclude that the agreement between the computations and experimental data indicates that our neglect of streamtube expansion and transverse mass diffusion are complementary. In real flames, it is thus likely that diffusion of reactants from the cool wall regions to the high-temperature regions behind the wave is counteracted by the lateral expansion of the combusted gas until far downstream where streamtube contraction starts to occur due to wall heat losses.

References

[1] Hirschfelder, J. O., Curtiss, C. F., and Campbell, D. E., "The Theory of Flame Propagation. IV," *Journal of Physical Chemistry*, Vol. 57, 1953, pp. 403-414.

[2] Spalding, D. B., "The Theory of Flame Phenomena with a Chain Reaction," *Philosophical Transaction of the Royal Society of London*, Vol. A249, 1956, pp. 1-25.

[3] Spalding, D. B., Stephenson, P. L., and Taylor, R. G., "A Calculation Procedure for the Prediction of Laminar Flame Speeds," *Combustion and Flame*, Vol. 17, 1971, pp. 55-64.

[4] Dixon-Lewis, G., "Flame Structure and Flame Reaction Kinetics I. Solution of Conservation Equations and Application to Rich Hydrogen-Oxygen Flames," *Proceedings of the Royal Society of London*, Vol. A298, 1967, pp. 495-513.

[5] Bledjian, L., "Computation of Time-Dependent Laminar Flame Structure," *Combustion and Flame*, Vol. 20, 1973, pp. 5-17.

[6] Wilde, K. A., "Boundary-Value Solutions of the One-Dimensional Laminary Flame Propagation Equations," *Combustion and Flame*, Vol. 18, 1972, pp. 43-52.

[7] von Karman, T. and Millan, G., "Thermal Theory of a Laminar Flame Front Near a Cold Wall," *Fourth Symposium (International) on Combustion*, Williams & Wilkins, Baltimore, Md., 1953, pp. 173-177.

[8] Penner, G. R., "An Investigation of Flame Stabilization Using Finite Difference Numerical Techniques," Ph.D. Thesis, University of Toronto, Toronto, Ont., Canada, 1973.

[9] Williams, F. A., *Combustion Theory*, Addison-Wesley, Reading, Mass., 1965.

[10] Aly, S. L., "A Two Dimensional Laminar Flame Theory: A Numerical Technique and Flame Quenching," Ph.D. Thesis, University of Waterloo, Waterloo, Ont., Canada, 1977.

[11] Gray, B. F. and Yang, C. H., "Boundary Conditions of the Downstream Singularity in Non-adiabatic Flames," *Combustion and Flame*, Vol. 10, 1966, pp. 199-200; ibid., Vol. 11, 1967, pp. 441-442.

[12] Adler, J., "Downstream Boundary Conditions of Non-adiabatic, One-Dimensional, Laminar Flames," *Combustion and Flame*, Vol. 11, 1967, pp. 85-86; ibid, Vol. 11, 1967, pp. 442.

[13] Stine, W. B., "On the Theory of Flammability Limits," Ph.D. Thesis, University of Southern California, Los Angeles, Calif., 1972.

[14] Buckmaster, J., "The Quenching of Deflagration Waves," *Combustion and Flame*, Vol. 26, 1976, pp. 151-162.

[15] Potter, A. E. Jr., "Flame Quenching," *Progress in Combustion Science and Technology*, Vol. 1, 1960, pp. 145-181.

[16] Yang, C. H., "Burning Velocity and the Structure of Flames Near Extinction Limits," *Combustion and Flame*, Vol. 5, 1961, pp. 163-174.

[17] Lieberstein, H. M., "A Numerical Test Case for the Nonlinear Overrelaxation Algorithm," University of Wisconsin Mathematics Research Center, Madison, Wis., MRC-TR-80, 1959.

[18] Swarztrauber, P. and Sweet, R., "Efficient Fortran Subprograms for the Solution of Elliptic Partial Differential Equations," National Center for Atmospheric Research, TN/IA 109, 1975.

[19] Roach, P. J., *Computational Fluid Dynamics*, Hermosa Publishers, 1976.

[20] Curtiss, C. F. and Hirshfelder, J. O., "Integration of Stiff Equations," *Proceedings of the National Aeronautical Society*, Vol. 38, 1952, pp. 235-243.

[21] Frank-Kamenetski, D. A., "Diffusion and Heat Exchange in Chemical Kinetics," Princeton University Press, Princeton, N.J., 1955.

[22] Hermance, C. E., "Implications Concerning General Ignition Process from the Analysis of Homogeneous, Thermal Explosions," *Combustion Science and Technology*, Vol. 10, 1975, pp. 261-265.

[23] Payman, W. and Wheeler, R. V., "The Propagation of Flame Through Tubes of Small Diameter," *Journal of Chemical Society*, Vol. 113, 1918, pp. 656-666.

[24] Botha, J. P. and Spalding, D. B., "The Laminar Flame Speed of Propane/Air Mixtures with Heat Extraction from the Flame," *Proceedings of the Royal Society of London*, Vol. A225, 1954, pp. 71-97.

[25] Spalding, D. B., "A Theory of Inflammability Limits and Flame Quenching," *Proceedings of the Royal Society of London*, Vol. A240, 1957, pp. 83-100.